Lund University

Report from internship in the nuclear division

Characterisation of a square-type HPGe crystal and development of the Lund germanium detector scanning system

Author:
Guillem Tocabens

Supervisors:
Luis Sarmiento
Dirk Rudolph
Anton Roth

June 21, 2017

Lund University

Abstract

This report was written as part of a project work carried out in the Nuclear Division of the Physics Department in Lund University. The objective of this project was to assist a PhD student, Anton Roth, in building a scanning system and studying a new type of Hyper Pure Germanium, HPGe, crystal. The report contains two main parts, the building of the scanning system and the characterisation of the crystals. For the scanning system, the principal result is the design and building of the positioning system. It was designed to hold the source collimator and direct the beam from above towards the detector, as well as moving it on the plane parallel to the ground. Two linear units were used, both fixed on the other one, to move the collimator in two directions and a linear guide was placed parralel to one linear unit to hold the weight of the collimator. The resolution of two crystal prototypes were determined and the effects of trapping and the inner capacitance of the crystal were studied. The main result of this study is that the effects of trapping are more important than the effects of the capacitance of the crystal, on the resolution of the detector. This implies that the length of the inner contact must be relatively long in order to minimise the average charge carrier path lengths and thus minimise the probability of trapping.

Contents

1 Introduction

Nuclear structure continues to be an active branch in the field of nuclear physics, because there is still a lot to discover. One of the things that is recognized among the nuclear physics' researchers is the existence of magic numbers. Nuclei having a magic number of protons, neutrons or both are usually more stable than neighboring nuclei, at least if nuclei not far away from the line of stability are considered (see Figure 1). Today, those numbers are known up to a certain point. Indeed, nuclei with $N, Z = 2, 8, 20, 28, 50, 82$ and $N = 126$ are more stable than others. Nevertheless, as soon as heavier nuclei (in the sense of nuclei with more protons and/or neutrons) are considered, no magic number of protons or neutrons have been experimentally observed. Theoretically some models are being developed and predict, for example, that $N = 184$ and $Z = 114$ could be the next magic numbers for neutrons and protons, respectively [1]. The search for an "island of stability" in the region of superheavy elements, having more than 103 protons, is thus very important to get the chance to observe stable (regarding spontaneous fission) superheavy elements, or higher levels of stability.

This process of researching the island of stability is not straightforward at all and requires at least two different steps. First of all, these superheavy elements need to be created. One widely used technique is via fusion-evaporation reactions : a beam of stable isotopes is accelerated towards a target made of a different element, typically heavier. The elements can fuse if the energy is larger than the Coulomb barrier. The fusion product evaporates neutrons, protons or other light particles, such as α particles [2], [3]. This way, heavy and superheavy elements can be created, such as in an experiment conducted in 2012 at the Helmholtz Centre for Heavy Ion Research (GSI, in Germany) by the Lund Nuclear structure group. A beam of ^{48}Ca was accelerated towards a target of ^{243}Am to create an element containing 115 protons recently named moscovium, Mc [4]. The creation process of superheavy elements is tedious since the cross sections for fusion-evaporation reactions are ridiculously little. In former experiments, only a few number, 30 for the one conducted in GSI in 2012, of nuclei of element 115 where observed.

The second step in the search for the island of stability actually contains two different processes which are closely linked : observation through decay and identification of the created element. Even though the elements which are looked for are stable against spontaneous fission, they still decay rather quickly through α decay. Half-lives, $T_{1/2}$, of known element 115 isotopes are on the order of hundred(s) of milliseconds, for instance. The emitted α particles can be detected and their energy can be extracted to reconstruct the α-decay chain originating from a specific isotope. But as the knowledge about superheavy elements is far from complete, it is hard to place that chain on the chart of nuclides and hence determine what element was created in the first place. Nonetheless, after emitting an α particle, nuclei from superheavy elements can end in an excited state of the daughter. The element may then decay to its ground state through electron capture decay that emits X-rays of some hundreds of keV (decay into the atomic K shell) or some tenths of keV (decay into the atomic L shell) for example. X-ray energies are specific to each element. Therefore, if they are detected a short time (some nanoseconds or less) after the alpha particle was detected, the term used is "in prompt coincidence", it is possible to identify the corresponding element. If this happens, the α decay chain can then be identified and, consequently, the created element too.

In the past decades, new superheavy elements were discovered, up to element $Z = 118$, Oganesson Og, first synthesized in 2002, confirmed in 2015 and finally named in 2016 [5]. In the perspective of finding the next superheavy element, $Z = 119$, new detectors must be developed where an advantageous feature would be high resolution in the X-ray domain. This report concentrates on the characterization of such a new system which should have a high resolution in both γ-ray domain (up to some MeV) and X-ray domain. Indeed, this detector will also be used to study known superheavy elements and determine their structure and decay.

The studied detector is a semiconductor detector using a high-purity germanium crystal with coaxial geometry. The main difference with usual germanium detectors is that while coaxial detectors are cylindrical, the new detector will have a cubic geometry. Computer simulations were performed to determine the right geometry to use for the detector configuration but also to determine how to pack four crystals into a "clover" of four detectors. However, the main topic of this report is to characterize the new detector by means of a scanning system. This system would be used to study the response of

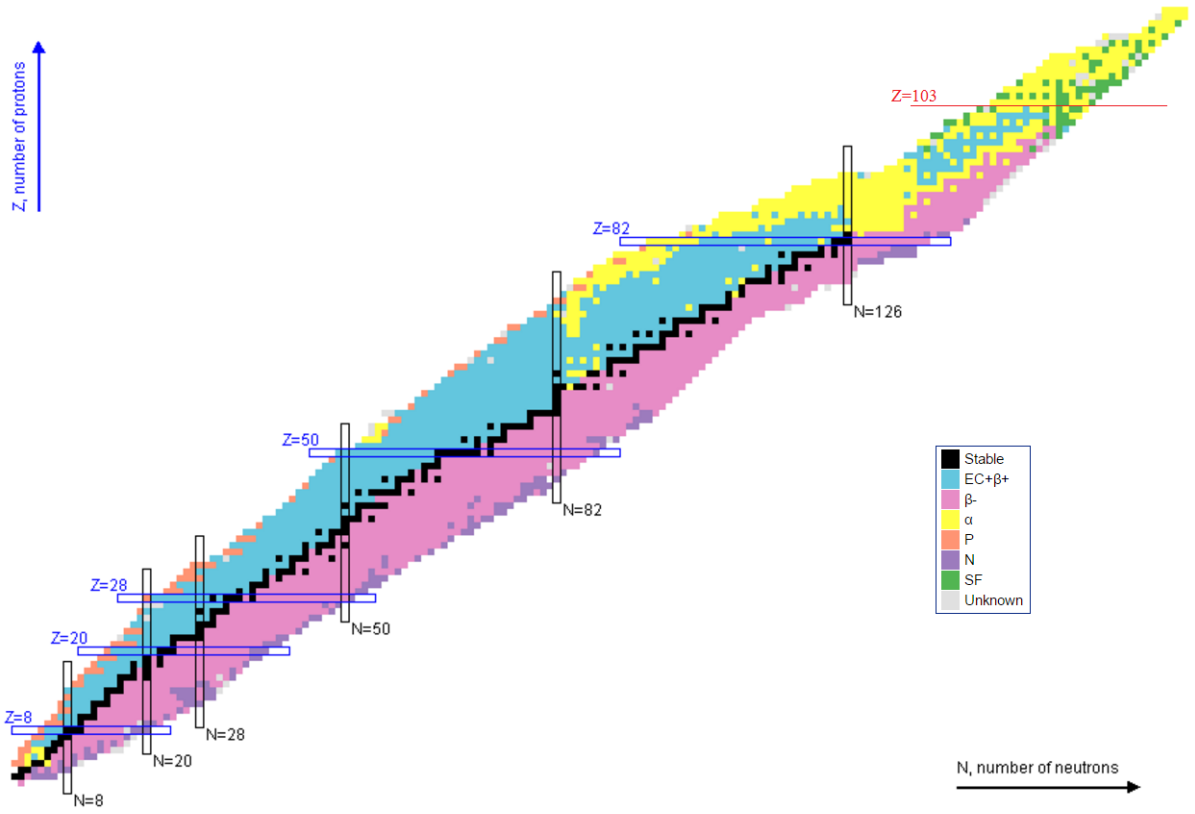

Figure 1: Chart of nuclides, classifying the nuclides with respect to their number of protons and neutrons. The known magic numbers are given on the chart as long as the nuclei having a magic number of protons, in blue, or of neutrons, in black (open rectangles). On that chart the colors represent the modes of decay of each nuclide, emphasized by the small squares. The region of interest is the one of the superheavy elements, up from the red line on the chart.

the crystal to a collimated beam at a given number of points of its surface. The whole functioning of the system is developed in this report.

But before being able to scan the crystal, the main part of the project was to build a setup that could match the needs of the experiments that would be performed with the detector. The goal here was to develop everything, starting by drawing the setup as it should look like in the end, purchasing all the needed material and pieces, and finally building the whole setup once the pieces were available.

Section 3 is dedicated to explain the development of this system and the different steps of the process while Section 4.4 presents measurements performed with two different prototypes of detectors. A background of the physics used in the report is introduced in Section 2 but it is assumed that a basic knowledge on semiconductor detectors is already in the hands of the reader.

2 Theory and background

2.1 The crystal

The studied crystal has the same characteristics as coaxial crystals, the only difference being its cubic geometry while coaxial crystals have cylindrical geometry. The crystal is a closed-end coaxial crystal, meaning its geometry is cubic with a hole in it that does not penetrate in the volume (see Figure 2). The crystal is oriented such that the incoming photons hit the part without the hole first. As photon interactions can only be detected within the depletion zone [6], a germanium crystal based detector must contain a p- and n-doped faces. The p-contact is made by adding an electron donor, here boron is implanted on the outer surface of the germanium crystal, and the n-contact is made by adding a hole donor, lithium, on the inner surface (the surface of the hole) of the crystal. Both these added layers function as dead layers[1] and affect the detection efficiency on the doped sides since the layer is measured to be 0.5 mm to 1 mm thick.

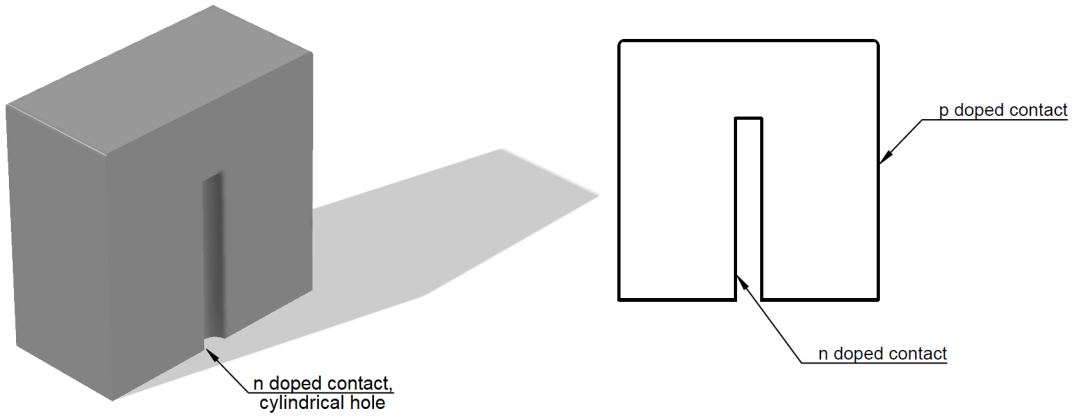

Figure 2: 3D view (left) and cut view (right) of the cubic prototype crystal.

In order to protect the crystal from oxidation, a passivation layer is added on the inner surface of the crystal. This layer is made with SiO_2, which is not optimal for germanium crystal as both crystal lattices does not fit. This could imply perturbations in the electric field, increasing noise in the measurements. To prevent from this potential noise, a methanol passivation [7] should be preferable on germanium or other silicon films [8]. However, such a passivation layer can't be achieved in atmosphere, but could be done in the encapsulation.

The crystal is placed in a cryostat that ensures its temperature to be as low as possible with liquid nitrogen as germanium detectors need to be cooled down to work properly [9]. The cooling is performed with a dewar filled with liquid nitrogen that is connected to the crystal through a cooling finger. Close to the cryostat is a preamplifier that converts the signal from current to voltage and amplifies it a first time [10]. The preamplifier is then the output of the detector which can be connected to further electronic devices.

2.2 Spectral properties

After going through different electronic modules, the signal detected by the crystal is sent to a computer to be analyzed. The collected data presents a number of counts detected by the crystal for each channel in the multichannel analyzer[2]. As a channel number is not really relevant for measures, the detector needs to be calibrated using a known source in order to associate an energy to each channel. The result is then a plot of the detected number of counts for each given energy which is called a spectrum. These spectra are of main importance as they allow to determine some of the spectral properties of the crystal and to study the nuclear structure properties.

[1] A dead layer is a volume that does not contribute to the detection of photons since it is not part of the depletion zone, due to its too high level of impurities.

[2] A multichannel analyzer, MCA, sorts the digital values it receives from an analog to digital converter, ADC, and stores them to be used on a computer.

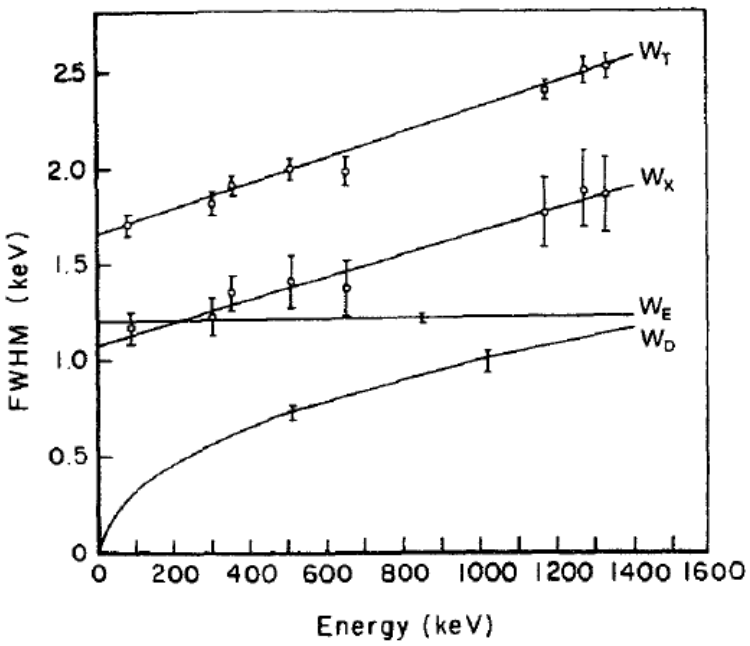

Figure 3: Plot of the different contributions to the energy resolution of a germanium detector as a function of the energy of the detected photon, image taken from Ref. [9].

The first property that is interesting to determine is the resolution of the detector as it gives the uncertainty on the measures performed with the detector. The resolution is determined by fitting Gaussians to the peaks in the spectra and calculating their Full Width at Half Maximum, FWHM, which is directly a measure of the uncertainty on the energy and thus the resolution of the detector. Resolution varies with the energy of the detected photon and is usually better in the low-energy range than in the high-energy range. Resolution can be written as the sum of three different contributions [10] :

$$W_T = W_D^2 + W_X^2 + W_E^2 \tag{1}$$

where the W are the expected peak FWHM due to charge carrier statistics, collection and electronic noise, respectively. While the contribution of electric noise is constant as a function of energy, both other contributions are energy dependent. W_D, the inherent statistical fluctuation in the number of created charge carriers varies with the square root of the energy of the detected photon while W_X, due to incomplete charge collection, varies linearly with energy (Figure 3).

Another important feature that can be determined from a spectrum is the shape of the peaks. While peaks are fitted to Gaussians, it is quite important to make sure that this approximation is true. In order to determine this, shape factors are often used. They are estimated using the ratio between the FWHM of the peak and the Full Width at Tenth Maximum or the Full Width at Fiftieth Maximum. Considering a perfect Gaussian peak, these ratios are given by :

$$\frac{FWTM}{FWHM} = 1.82 \text{ and } \frac{FWFM}{FWHM} = 2.38 \tag{2}$$

The shape depends on the electronics (too short shaping time, bad pole-zero adjustment, etc.) but can also be affected by other factors such as damages on the crystal or a too high count rate leading to pile-up.

2.3 Capacitance

As a result of the electric field present in the depletion region of a germanium detector, the crystal shows an inherent capacitance. This capacitance varies with the voltage applied to the crystal and is constant when a sufficiently high voltage is applied on the crystal. In a reversed bias regime, the

capacitance decreases when the absolute value of the voltage increases thus, to make the capacitance as low as possible, the reversed bias applied to the crystal must be as high as possible. It is important to have a low capacitance in the crystal while it is one of the reasons for electric noise on the spectra. Indeed, the noise charge, which is a measure of the noise level, is proportionnal to the total capacitance in the detector. The total capacitance comes from the electronics but also in part from the crystal. Hence, it is important to minimise the capacitance in the crystal to obtain as little noise as possible and a good resolution [11].

The capacitance of a semiconductor crystal only depends on its geometry. In the case of a cubic crystal, the calculation had not been made but qualitatively it can be said that the capacitance is larger when the hole in the middle of the crystal is larger. The hole must then be kept as shallow as possible to get a reasonable resolution. As will be discussed further, the capacitance is not the only factor that influences resolution and trapping can be a big issue.

2.4 Trapping

Trapping is an important issue when it comes to resolution in germanium detectors as it is contained in the W_X term (see 2.2) corresponding to charge carrier collection. Due to the impurities and the defects in a germanium crystal, new energy states appear that can trap the electrons (or holes). When a charge carrier is trapped in such a state, there are two different possibilities :

- If the trapping center can trap both types of charge carriers (electron and holes), it could occur that a second charge carrier is trapped, anihilating both and implying a loss in carriers.
- If the trapping center can only trap one of the two types of charge carriers, the trapped carrier will stay in the trapping center for a given time and then continue its path to the collection center.

The first possibility ends up with a loss in charge carriers and thus a loss in energy resolution. For the second possibility, there are again two possible scenarios. Either the trapping time is shorter than the collection time and thus the carrier is released before the end of the collection and can still participate in the signal. In the case of a longer trapping time than the collection time, then the carrier does not participate in the signal, resulting in a loss of energy resolution and a poor shape of the peaks in the spectra [10].

Of course, the number of trapped charge carriers depends on the number of impurities in the crystal. The concentration of trapping centers should not be higher than $10^{10}\ cm^{-3}$ [12] and hence the concentration of impurities should be of the same order as the number of trapping centers to avoid trapping as much as possible. In the case of the studied prototype, as it has a cubic geometry, all the charge carriers do not have the same path length to travel to the collection center in the middle of the crystal. A longer path would result in a higher probability for a charge carrier to be trapped. Thus, the length of the hole in the middle of the crystal, which is the collection center, is of primary importance to reduce the effects of trapping. With this property of trapping, a poorer resolution is also expected for γ-ray interactions occuring in the corners of the crystal compared to the middle since the path length is again increasing. This shows the importance of scanning the detector on its volume in order to improve the resolution by optimizing the analysis routine.

Finally, the amount of charges that are trapped in the trapping centers depends on the energy that is deposited in the detector. The effects of trapping are more important for higher energies. This is also something that will be discussed in section 4.4 with respect to the measurements that were performed on two different prototypes of detectors.

3 Scanning system

This section presents the reasoning and building of the scanning station by going piece by piece and discussing the needs of each piece as well as the problems encountered. The section is illustrated by pictures of the setup, mostly by 3D drawings made using a 3D drawing software since the setup was not mounted at the end of the project.

3.1 Aim of the setup

The main goal of the scanning station is to be able to scan a crystal in all the directions in space. To achieve this, the scanning process will be performed measuring coincidences between the crystal and LYCCA [13] modules surrounding it. This technique allows to determine where the interaction took place in the crystal in the vertical direction while the radioactive beam is collimated on top of the crystal and moved in order to scan it on a horizontal plane. This way, the crystal can be scanned in all directions in space to allow optimizing the analysis routine afterwards. For example, a shift in energy between an interaction occuring in the corner and in the middle of the crystal can be compensated by the means of a pulse shape analysis. The station was built starting from zero and trying to match as good as possible the requirements and minimize the risks of any breakdown of the system. The final idea of the setup is presented in Figure 4 where a 3D drawing of what it should look like is presented. This section of the reports concentrates on explaining the approach of building the entire scanning station layer by layer.

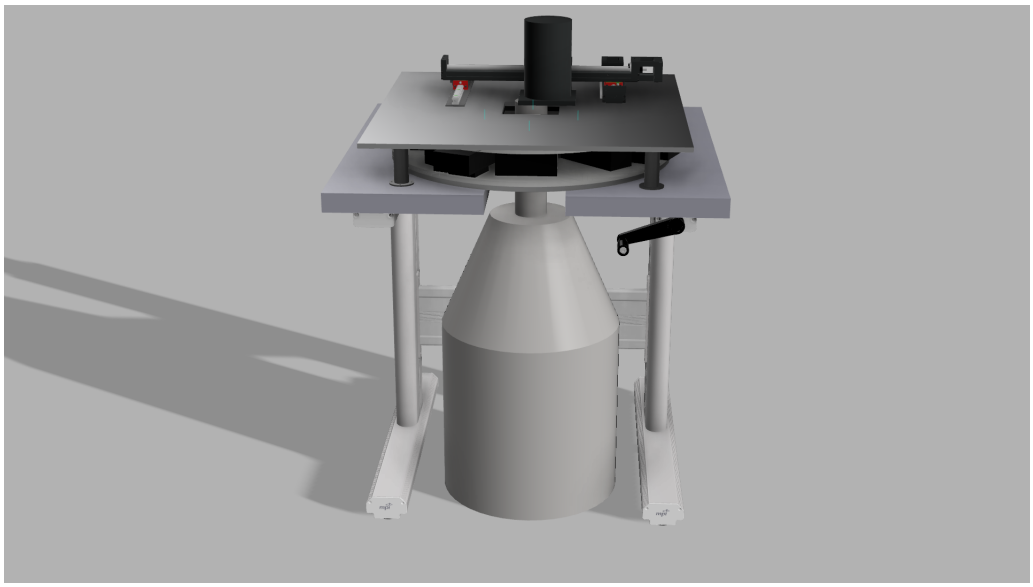

Figure 4: 3D view of the final scanning station. From top to bottom are shown the x-y scanning system with the collimator (black cylinder), the LYCCA ring (coincidence setup) between the top table and the adjustable table and finally the dewar holding the crystal in its upper part (grey cylinder).

3.2 Coincidence setup

The coincidence setup is made of a ring containing 12 LYCCA modules surrounding the crystal to determine the vertical position where the interaction took place. Horizontal absorbers made of tungsten are placed between the crystal and the modules to enable only some coincidences to be detected in the zones between two absorbers (see Figure 5). The crystal is placed in the middle of the ring and the collimated beam is directed from above towards the crystal.

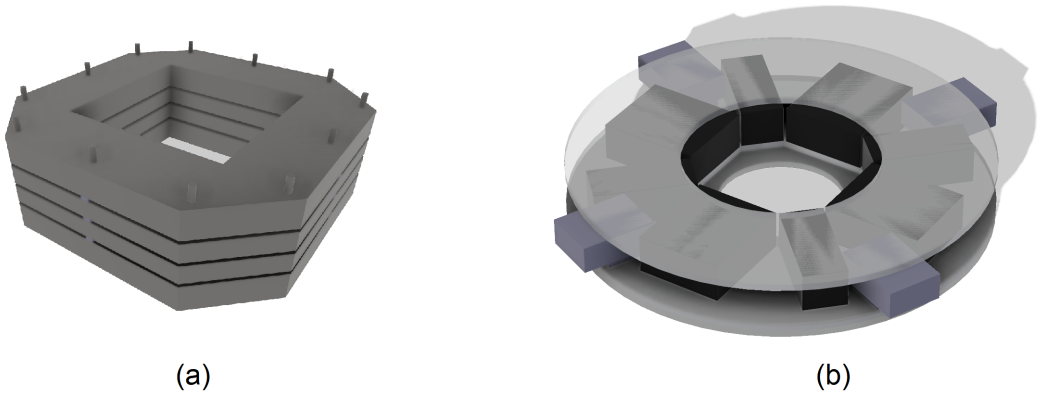

Figure 5: 3D views of the tungsten absorbers, (a), and the LYCCA ring, (b). On figure (a), each absorber is separated by little plastic pieces (in blue) to have a space where the coincident photons can be detected by the LYCCA modules. The LYCCA ring is made of twelve modules (black boxes) powered by four preamplifiers (blue boxes). The absorbers are mounted in the middle of the ring and the beam is directed towards the squared hole.

3.3 The holding structure

This part of the setup was rather complicated to develop since some major constraints have to be taken into account. The first constraint is that the dewar must fit under the table while the crystal must be protruding above its plate to allow the coincidence setup to be mounted on the table. The solution here was to design a table with a hole in the middle allowing this as can be seen on the final design of the table, Figure 6. Another constraint was to have a height adjustable table. Indeed, the coincidence setup could not cover the whole crystal to be scanned in height, having a height adjustable support for it could make a scan on the whole vertical direction of the crystal possible.

Finally, the loading capacity of the table should be sufficiently high while some pieces such as the horizontal absorbers (3.2) and the collimator are made of tungsten for a global weight of around 60 to 70 kilograms, without counting other pieces, the total weight being estimated around 100 kilogramms. A 3D view of the table is shown in Figure 6. On this first layer, the LYCCA ring will be mounted in the middle to match with the end of the cap coming from the dewar.

The next step was to find a solution in order to put the xy-scanning system on top of the table. Again, this second layer should be quite resistant as a load of around 30 kilograms would then be added on top of it. In order for the directed beam to reach the crystal, a hole should be drilled in the middle of the top plate, matching the dimensions of the crystal to scan. As the bottom table is already height adjustable, this second layer did not need to be as well, reducing the constraints. For all these reasons, a thick plate of iron with a square hole in the middle was designed to be mounted on four legs fixed on the table in the four corners. The result presenting the structure of the setup is shown on Figure 6.

3.4 The xy-scanning system

After the global structure of the scanning station was decided, certainly the most critical step was to develop the xy-scanning system. Indeed, this construction had to fulfill several conditions such as a rather good uncertainty on the positionning, the possibility to remotely control the movement, a quite high load capacity, etc. After some research and calls to different companies, the best option seemed to use two linear units and a linear guide and hang the collimator containing the source on one of them (see Figure 7). Linear units are devices that contain a rail and a wagon and use a screw going through the wagon to move it with a motor. Thus, a linear unit can move its wagon in one given direction. Therefore, fixing two of those units on one another and perpendicular to each other should allow an object fixed on top to move in two different directions. The linear guide, which has basically the same role as the linear units except it is not motorized and then just follows the lead, is placed parallel to the

Figure 6: 3D view of the table and the top plate. The dewar and the cryostat containing the crystal are also represented as they should go in the final setup. The coincidence setup (absorbers and LYCCA ring, 3.2) fits between the table and the top plate to collect 90° scattered photons from the crystal. The xy-scanning system (3.4) is fixed on top of the plate.

first linear unit so that the one on top can be fixed to both, increasing the stability and load capacity of the construction.

The whole scanning system needs to be mounted on top of the principal structure so that the radioactive beam can be directed towards the crystal. As the linear units and the linear guide have holes, matching holes were drilled in the top plate at the correct positions in order to be able to cover the square hole in the middle of the plate. The last concerns about the units were to obtain a correct precision in their movement and to be sure that they could hold the collimator. The precision is only limited by the motors used to move the wagons, while the precision of the units is of the order of some microns, way better than what is needed here, as 0.1 mm seems reasonable. Thus the motors were chosen to match this requirement and to be powerful enough to push the wagon with the collimator (around 26 kg). For the load, the linear units are not supposed to hold a great vertical load, but they can support a high torque in any direction. An arm protruding from the top unit was then designed to hold the collimator. This would minimise the vertical load applied on the wagon and maximise the torque, making this solution viable.

The collimator arm was the last piece of the setup to be designed and its ideal shape was quite hard to determine. The first thought was to build it as a stair, with the upper step being fixed on the wagon and the lower one holding the collimator. As the collimator is quite imposant and extremely dense (tungsten alloy to collimate the beam in a 1 mm hole going through it), a back-up plan was designed using two spherical wheels on an extension of the arm that would allow the collimator to rest on the top plate, distributing the load on it (see Figure 8). To study the need for this extension, stress simulations were performed for two principal materials, aluminum and steel. The results, estimated for a load of 30 kg applied on the whole lower step, showed a maximum vertical deformationof around 0.3 mm for aluminum and 0.1 mm for steel. Such a deformation would lead to an uncertainty on the position of the beam on the crystal of 0.1 mm and 0.05 mm using aluminum and steel respectively. The solution that was kept was thus a steel arm, as shown on Figure 8 and the back-up plan with the extension was still kept in mind if the first tests with the regular arm were not satisfying.

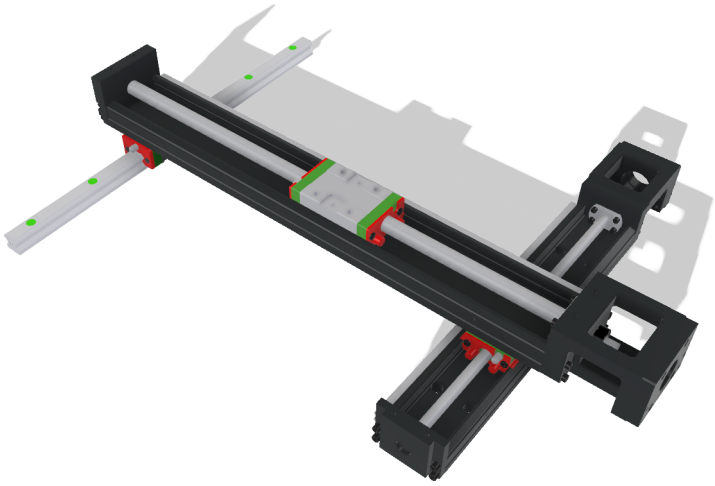

Figure 7: 3D view of the xy-scanning system. The linear guide (grey) and linear unit (black) under are fixed on the top plate and allow a movement in one direction. The collimator arm with the collimator are fixed on the wagon of the linear unit on top which allows movement in the other direction.

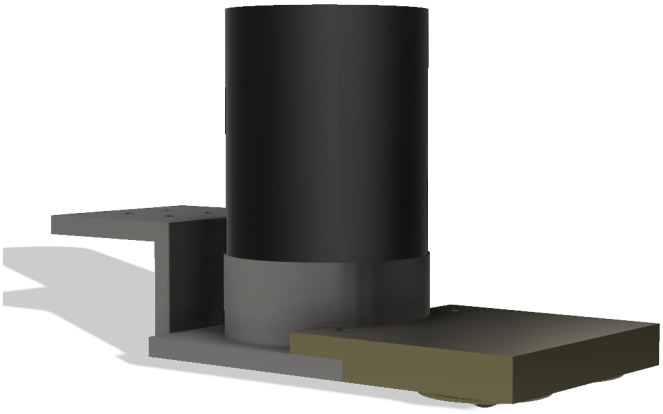

Figure 8: 3D view of the arm holding the collimator (black). This 3D drawing shows the arm as it was first designed (grey part) and with an extension (golden part) that could be added in case the linear unit could not bear the collimator (this part was finally not needed).

4 Scanning the prototype detector

While the scanning station was not already built and the different pieces took several months to arrive to Lund, measurements were performed with another setup that used material available in Lund. This was made to verify the measurements of resolution given by the company building the prototypes of detector, Canberra. These first measurements were also an opportunity to study the effect of capacitance of the detector and trapping on the resolution and compare both effects.

4.1 Overall setup

The setup uses three detectors: two scintillator detectors, placed on the sides (black squared boxes in Figure 9) and one semiconductor detector - hyperpure germanium detector - below the collimated source (grey cylinder in Figure 9). The source is placed on the top lead brick which contains a hole in the middle to collimate the radioactive source. In that position, the source is 97mm from the top of the crystal, which is 5mm from the top of the cryostat, and collimated in a 5mm hole through an 80mm lead brick. The source is covered by a little lead brick and the setup is shielded by lead to avoid propagation of gamma radiation away from the setup (see Figure 10).

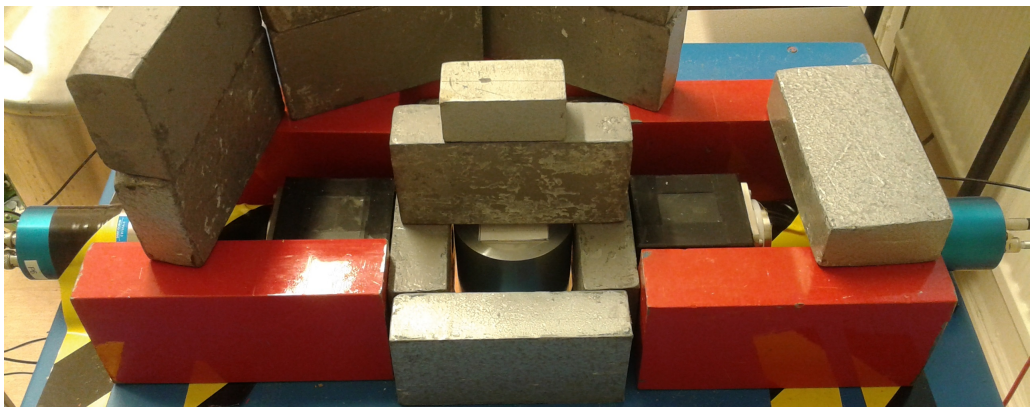

Figure 9: Back of the original setup. The scintillator detectors are the black squared boxes on the sides of the germanium detector, placed in a cryostat (grey cylinder in the middle).

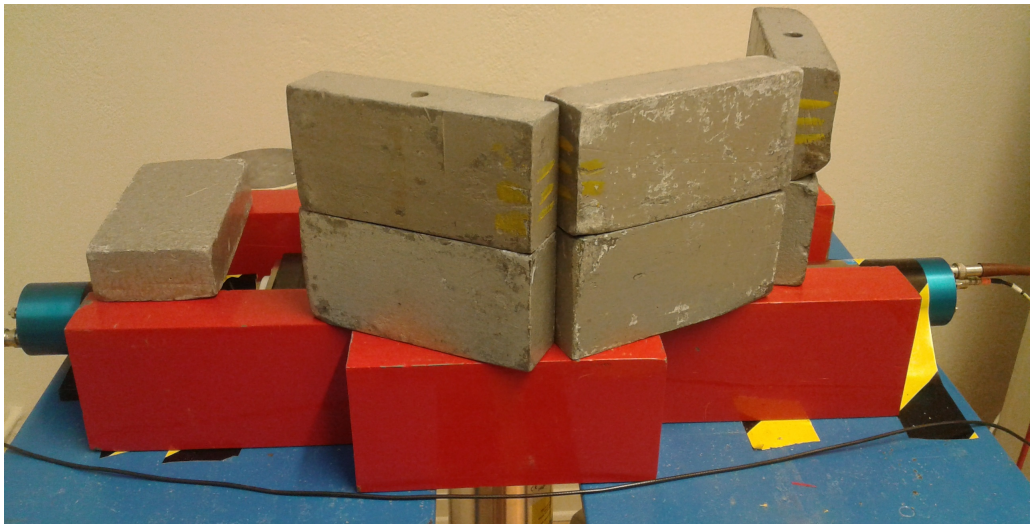

Figure 10: Front side of the original setup (with the lead shielding). Two holed lead bricks can be seen on this picture as the one used to obtain a collimated beam.

4.2 Process of measurement

For the first set of measurements, only the germanium detector was used and not the scintillator detectors. The goal of this experiment was to determine some spectral properties of the detector depending on the location of the collimated source such as the resolution of the crystal. Therefore, the source was directed onto five different points on the top of the crystal: one measurement was performed directing the beam in the center of the crystal surface, and four in the corners of the crystal surface. This was made possible by the use of a holed lead brick on top of which the source was positioned. The scanning was conducted as described below and two different cobalt sources were used, one of ^{60}Co and one of ^{57}Co.

In the case of ^{60}Co, the source was held in one of the positions until the net area[3] of the studied peak (peak at 1332 keV) contained at least 100 000 counts to match the measurement performed by the company manufacturing the detectors. Since the ^{57}Co source was much less active, the measurement was stopped when the net area of the studied peak (peak at 122 keV) contained around 1 000 counts.

The very first step was to perform the calibration. To do so, the two lines present in the spectrum of ^{60}Co were used (lines at 1173 keV and 1332 keV) and associated to a channel in the 8192 channel analyzer. In order to avoid a shift in the low energy range, the line at 122 keV in the spectrum of

[3]In the analysis of the spectra, two areas need to be differenciated : the total area, which gives the total number of counts between two channels, and the net area, which gives the number of counts between two channel substracted by the background.

^{57}Co was also used. Then a linear fit was performed to get the the calibrated energies and then the equation of channels as a function of energy that was used in the analysis procedure later on (the data analysis is described in section 4.4).

4.3 Electronics

For the first set of measurements, the scintillator detectors and the coincidence setup were not used, thus the electronics are relatively simple. The germanium detector is powered by a high voltage supply as explained in section 2. After going through a preamplifier, included in the cryostat, the signal is sent to an amplifier. Besides amplifying the signal, the amplifier also shapes it to a Gaussian. It is then digitized by an Analog to Digital Converter, ADC, and a multichannel analyzer sorts the digital values which are sent to the computer that collects the data using the Maestro software. Both the high voltage supply and the amplifier are Nuclear Instrumentation Modules (NIM, a standard set of modules) and are placed in a NIM crate that provides the necessary power for operation.

4.4 Results and analysis

4.4.1 First prototype

The measurements that were conducted here had two main objectives. First, they were done in order to verify the values of the principal characteristics claimed by Canberra but this first experiment was also performed to get a first idea of how the crystals will be scanned with the final scanning system and what quantities to measure. The detector was scanned following the protocol explained in section 4.2.

The resolution of the detector, given by the full width at half maximum (FWHM), along with the shape of the peak, emphasized by the ratios between, the full width at tenth and fiftieth maximum, and the FWHM, were studied. The results are shown in the two tables below, both for the ^{60}Co and ^{57}Co source (Tables 1 and 2). For each source, the peaks in the spectra were fitted with Gaussians and the FWHM was deduced from the fit. As the fitting program uses the FWHM to optimise the fit, the value given by the Gaussian fit is the same as the real value of the FWHM that can be read from the data. This is not the case when it comes to the FWTM and FWFM and these values were directly read off the spectra without using the fit.

Table 1: Recap-table of the obtained results for the first prototype using the ^{60}Co source. ^{60}Co and ^{57}Co were used for calibration to avoid possible shifts in the low energy range.

	Cobalt 60					
	Center	Top right	Bottom right	Bottom left	Top left	Mean
Energy (keV)	1332.46	1331.97	1331.86	1331.69	1332.18	1332.03
FWHM (keV)	2.50	2.77	2.88	2.99	2.63	2.75
FWTM/FWHM	1.88	1.90	1.92	1.91	1.90	1.90
FWFM/FWHM	2.54	2.52	2.46	2.45	2.54	2.50

Table 2: Recap-table of the obtained results for the first prototype using the ^{57}Co source. ^{60}Co and ^{57}Co were used for calibration to avoid possible shifts in the low energy range.

	Cobalt 57					
	Center	Top right	Bottom right	Bottom left	Top left	Mean
Energy (keV)	122.05	122.24	122.17	122.16	122.23	122.17
FWHM (keV)	1.58	1.56	1.58	1.63	1.58	1.59
FWTM/FWHM	1.80	1.95	1.90	1.89	1.95	1.90
FWFM/FWHM	2.27	2.45	2.54	2.29	2.35	2.38

The very first thing we can notice in this set of measurements is that there is a shift in energy depending on where the beam was collimated. This shift in energy between the expected values [14] and the measured values goes up to around 0.8 keV if the beam is not directed towards the center of

Table 3: Values of resolution and symmetry ratio for the first prototype provided by Canberra.

	Cobalt 57	Cobalt 60
FWHM (keV)	0.81	2.40
Ratio FWTM/FWHM		2.19

the crystal. It is normal that the measure of the peak energy in the center of the crystal is the closest to the energy we can find in the literature, while the calibration was made using this measurement and the measurement in the center with a ^{57}Co source. This is also why the same measurement done in the center of the crystal with the ^{57}Co source gives the closest result to the literature value. The shift in energy is more important in the range of high energies and thus for the results obtained with the ^{60}Co source. This is exactly the expected result as shown in Section 2. Indeed, the effects of charge carrier trapping increase with the energy of the collected photon. Trapping causes losses in the energy resolution, the shape of the peaks and could also explain the observed shift in energy [15]. The fact that this shift also changes depending on where the beam is directed is interesting to notice. As stated in different articles treating the subject (see [15], [16] and [17] for instance), this could come from the difference of path the charge carriers need to travel depending if the interaction happens in a corner or in the center of the crystal. As seen before in Section 2, the more charge carriers have to travel to reach the electrodes and be collected, the more they are susceptible of being trapped in the crystal. This can imply a shift in energy and also differences in the measure of the resolution of the crystal as explained earlier.

A similar observation can be made when looking at the resolution measured in the different parts of the crystal : as for the peak energy, the resolution changes depending on the direction of the beam. The difference is not huge for measurements with the ^{57}Co source, but for the ^{60}Co source, the resolution varies from 2.50 keV up to 2.99 keV which is quite a big difference. Nonetheless, these values of resolution are roughly in agreement with the values provided by Canberra for the ^{60}Co, which were, for this first prototype, 2.40 keV at 1332.5 keV (see Table 3). The difference between both measurements in Lund and in Canberra can be explained by the different experimental conditions in which the measurements were done. The cryostat used with the crystal could influence the measured resolution, as well as the electronics and the treatment protocol of the data. While the first is not critical, an improvement in the electronics used can change the values of the resolution by quite a lot and as the program used to analyse the data was not the same in both cases, this could also influence the measured FWHM. What is relevant to notice here is the huge difference between the resolution obtained at Lund and at Canberra for the ^{57}Co source : 1.59 keV were measured in Lund, which means almost twice what was given by the company (0.81 keV). Appart from the fact that this measurement is far from the wanted final resolution in this range of energy, the difference between both measurements is quite important. This could be explained by the ^{57}Co source used in Lund : the source was too weak and the net area of 100 000 counts under the peak recommended by Canberra could not be reached. These values were measured with a net peak area of around 1 000 counts. The peak to background ratio was thus not as high as it should have and the resolution values were then not as good as Canberra claimed.

Finally, the symmetry ratios have been calculated and compared to the values given by Canberra (see Table 3). Again, for the ^{57}Co source, it may not make a lot of sense to look at those values, as the peak is not large enough to be analyzed in a proper way. The value obtained for the ^{60}Co source is closer to the theoretical value than the value given by Canberra (1.90 against 2.19), indicating that the peaks obtained on the spectra are closer to a Gaussian shape.

4.4.2 Second prototype

For the second prototype, the goal was just to perform the measurements to verify the values provided by Canberra for this prototype and the detector was not scanned as explained in 4.2. Instead, the source was just placed at the exact same distance from the cap as described in 4.1 but not collimated using a lead brick, in order to get a proper number of counts per second. Results are shown in Table 4 for the different sources that were used.

Table 4: Comparative table of the obtained resolution using, from left to right, ^{241}Am, ^{57}Co, ^{60}Co and ^{137}Cs. The cesium measurement was only performed in Lund in order to have values of resolution in the medium energy range and not just in the low and high energy range. ^{60}Co and ^{57}Co were used for calibration to avoid possible shifts in the low energy range.

Full width at half maximum	60 keV	122 keV	1332 keV	661 keV	
Measured resolutions in keV	0.71	0.81	2.10		Canberra
	0.74	0.88	1.91	1.45	Lund

In the three cases that were given by Canberra, the results were in agreement and there were no large deviations as observed for the first crystal. The low energy resolution was found to be way higher (decrease in the FWHM) than the one from the first crystal and overall the resolution improved quite significantly compared to the other detector. As for the first tested prototype, all these results are to be optimised using better electronics and cryostat as well as optimising the data analysis routine.

The symmetry ratios of the peaks were also determined and matched quite well the ones given by the company, again slightly better than the ones from the first crystal (Table 5). The difference between these values can also be explained by the use of different electronics, that could lead to a better peak shape even if the differences are not significantly high.

Table 5: Comparative table of the peak shape at 1332.5 keV from the ^{60}Co spectrum obtained with the second prototype.

	Canberra	Lund
Ratio FWTM/FWHM	1.95	1.90
Ratio FWFM/FWHM	2.80	2.76

The results for the resolution are quite interesting to analyze because the main difference between both crystals is the length of the hole in the middle, which is longer for the second prototype. As the capacitance of the crystal increases with the length of the hole, the resolution should decrease with the length of the hole getting longer (see section 2). This is however not the case and the behaviour looks exactly the opposite. One of the reasons for that could be that as the length of the hole is increasing, the mean path of the charge carriers to travel to the inner electrode is decreasing and thus trapping is getting less important. As discussed earlier, effects of trapping can be really important on both the count rate and the resolution of the detector. From these results it is possible to conclude that effects of trapping are more important than capacitance as resolution was better for the second prototype. Trapping is also a big problem when it comes to the shape of the peaks, as can be seen from the differences in the symmetry ratios obtained with both prototypes (Tables 1, 3 and 4). This also confirms the fact that trapping was affected by the length of the hole and that a longer hole is better to obtain a good resolution in this semiconductor detector. Nevertheless, a longer hole reduces the volume of collection of the crystal and thus its efficiency. The whole difficulty is thus to find the correct length of the hole to obtain the wanted resolution, taking into account both trapping and capacitance effects, and trying to have a reasonable efficiency by keeping a good volume of collection.

5 Conclusions

The building of the scanning system was the main part of this project and ended with the whole setup almost mounted. One of the hardest part in that work was to design the positionning system and the arm holding the collimator because of the different constraints. Indeed, the weight of the collimator made it difficult to model the arm and to create a solid system. In that purpose, the final system was composed of two linear units allowing a movement in two different directions by fixing them on one another. A linear guide was added parallel to one of the units to hold the weight of the unit on top and the collimator. With the help of two motors, the wagons on the units were able to be moved, pulling the collimator along to direct the beam towards any point on the surface of the detector. The creation of the arm needed to hold the collimator was delicate and a back-up solution was also designed to avoid breaking the system. Even if computer simulations were conducted to study the best shape for the arm, a big concern was if the linear units could bear the load. It ended up pretty well and when the pieces were available, the positionning system was mounted and shown operational. ~~The collimator could be moved using a computer program as the motors were connected to a Raspberry Pi. Finally, a stopping system was added to avoid any breakin the system. The system is rather simple and uses stoppers that kill the Raspberry Pi as soon as the collimator arm goes too close to the linear units.~~

The building of the setup was gratifying as it was possible to see everything being mounted after the 3D drawings were done and the research made. It was also interesting to start from scratch and build the setup piece by piece, discussing in the lab to think about the best solution.

Even if the system was not used to scan the detector prototypes, a first scanning was performed using lead bricks to collimate the beam towards the wanted points on the detector surface. The main result of this first scanning is the important role of charge carrier trapping in the germanium crystal that limits the resolution. As this effect is larger as the collection surface, the circular hole in the middle of the crystal, gets shorter, it was showed that a longer hole was preferable to obtain the wanted resolution. Even if the length of this hole also affects the inner capacitance of the crystal, this effect was determined to be smaller than the effect of trapping on both the resolution of the detector and the shape of the peaks in the final spectra.

This project was a great way to learn more about germanium detectors and showed interesting results. It allowed to compare the effects on resolution of trapping and conductance in this new type of semiconductor detector. Consequently, it showed that a longer hole was preferable as the effects of trapping were prevailing regarding resolution. It was also a good opportunity to study electronics that are used in usual nuclear physics experiments.

References

[1] A. Sobiczewski, F.A. Gareev, and B.N. Kalinkin. Closed shells for $z > 82$ and $n > 126$ in a diffuse potential well. *Physics Letters*, 1966.

[2] John Matti Nieminen. *Superdeformation : a tool to study fusion-evaporation reactions.* PhD thesis, School of Graduate Studies, 1998.

[3] Michael Thoennessen. *The discovery of isotopes, a complete compilation.* Springer, 2016.

[4] D. Rudolph et. al. Spectroscopy of element 115 decay chains. *Physical review letters III*, 2013.

[5] Vladimir Utyonkov, Yuri Oganessian, Sergey Dmitriev, Mikhail Itkis, Kenton Moody, Mark Stoyer, Dawn Shaughnessy, James Roberto, Krzysztof Rykaczewski, and Joseph Hamilton for the collaboration. The discovery of elements 113-118. In *Nobel Symposium on the Chemistry and Physics of Heavy and Super Heavy Elements.*

[6] William R. Leo. *Techniques for nuclear and particle physics experiments.* 1999.

[7] D.R. Napoli, G. Maggioni, S. Carturan, J. Eberth, M. Gelain, M.G. Grimaldi, S. Tati, S. Riccetto, and G. Della Mea. Germanium detectors for nuclear spectroscopy : current research and development activity at lnl.

[8] Changkun Xie, K. Michael Yocum, James F. Colaresi, and Harry S. Miley. Surface passivation of high purity germanium detectors using amorphous hydrogenated silicon films. *Monitoring Research Review: Ground-Based Nuclear Explosion Monitoring Technologies*, 2010.

[9] Glenn F. Knoll. *Radiation Detection and Measurement.* 1999.

[10] Nicholas Tsoulfanidis. *Measurement and detection of radiation.* Taylor & Francis, 1995.

[11] Jeremy D. Kephart. Method of evaluating the effect of hpge design on the sensitivity of physics experiments. Master's thesis, Graduate Faculty of North Carolina State University, 2009.

[12] ORTEC. *Review of the Physics of Semiconductor Detectors.*

[13] P. Golubev et. al. The lund-york-cologne calorimeter (lycca): Concept, design and prototype developments for a fair-nustar detector system to discriminate relativistic heavy-ion reaction products. *Nuclear Instruments & Methods in Physics Research. Section A: Accelerators, Spectrometers, Detectors, and Associated Equipment*, 2013.

[14] National nuclear data center. http://www.nndc.bnl.gov/.

[15] R. Trammell and F.J. Walter. The effects of carrier trapping in semiconductor gamma-ray spectrometers. *Nuclear Instruments and Methods*, 1969.

[16] M. Martini and T.A. McMath. Trapping and detrapping effects in lithium-drifted germanium and silicon detectors. *Nuclear Instruments and Methods*, 1969.

[17] Thomas W. Raudorf and Richard H. Pehl. Effect of charge carrier trapping on germanium coaxial detector line shapes. *Nuclear Instruments and Methods in Physics Research*, 1986.